

Supplementary Information

Accelerating the electron-transferring of nitrogen electro-fixation through assembling the Fe nanoparticles into Fe nanochains

Rongkang Wang,^{‡*a} Jingyu Lu,^{‡*b} Xu Li,^c Chunyu Song^a

^a Chongqing Chemical Industry Vocational College, Chongqing, 401228

^b School of Materials Science and Engineering, China University of Petroleum (East China), Qingdao 266580, China

^c Southwest Technology and Engineering Research Institute, Chongqing 401329, China

[‡] The authors contributed equally to this work

*Corresponding authors: E-mails: wrk1992@163.com; jingyulu1003@163.com

I. Experimental Section

1. Electrochemical characterizations

1.1 Electrode preparation: 5 mg of testing samples, 1 mg of acetylene black (conductive agent), and 30 μL of Nafion solution (5 wt%) were dispersed in 1 mL of isopropanol/DI-water ($v/v=4 : 1$) mixed solutions, which were ultrasonicated for 30 minutes (mins) to form a uniform catalyst ink. Next, 600 μL of the above catalyst ink was transferred to a $1.0 \times 3.0 \text{ cm}^2$ gas diffusion layer (GDL), where the effective catalytic area is $0.5 \times 2.0 \text{ cm}^2$ and mass loading is 1 mg cm^{-2} .

1.2 Electrochemical testing: Cathodic nitrogen reduction reaction (NRR) were studied in a three-electrode flow-type electrolytic cell under Ar- or N_2 -saturated conditions connected to a CHI 760E electrochemical workstation using the Fe nanochain or Fe nanoparticle as working electrode, GDL as counter electrode, Ag/AgCl (saturated KCl) as reference electrode, Nafion 115 membrane as the separator, 0.1 M Na_2SO_4 as electrolyte and 0.05 M H_2SO_4 aqueous solution as exhaust gas absorption chamber. The feeding rates of electrolyte and gas flow (N_2 or Ar) were 40 and 20 mL min^{-1} , respectively.

Note that Nafion 115 membrane may become the NH_3 contamination because it can absorb and release NH_3 . Therefore, it was sequentially pretreated in H_2O_2 aqueous solution (5 wt.%, 80 $^\circ\text{C}$) for 3 h, DI-water (80 $^\circ\text{C}$) for 1 h, 0.5 M H_2SO_4 solution (80 $^\circ\text{C}$) for 2 h, 0.5 M H_2SO_4 solution (100 $^\circ\text{C}$) for 8 h, DI-water (80 $^\circ\text{C}$) for 1 h and rinsed

in DI-water several times.

Before electrochemical test, the electrolyte was purged with Ar or N₂ flow (pretreated by 0.5 M H₂SO₄ and 1 M KOH aqueous solution) for 30 mins. During electrolysis, catholyte and anolyte are pumped through corresponding chambers separated by Nafion 115 membrane and pumped out separate reservoirs. N₂ gas enters the cathode chamber through the PTFE, and is captured on the surface of catalyst. The product is extracted and collected by acid absorption chambers isolated from external pollution, ensuring the accuracy of the experiment. To analyze NRR activities, linear sweep voltammograms (LSVs) was performed at a scan rate of 5 mV s⁻¹ in the potential range of -1.2~0 V (vs. RHE), and chronoamperometric test was carried out at different potentials for 1 h with continuous saturation Ar or N₂ flow in the electrochemical system. To avoid external pollutions, the electrolytes were prepared and used fresh, and the first cycle data is discarded. In order to analyze the mechanism of valence change of all Zn-MOFs at the reduction potential, cyclic voltammetry (CV) curves were tested at 0.3 to -1.2 V (vs. RHE).

The Tafel slopes were calculated according to the Tafel equation as follows:

$$\eta = b \log j + a,$$

where η is overpotential (V, calculated by $|E - E^* \text{ OER}|$), j is partial current density of NH₃ production (mA cm⁻²), and b is Tafel slope (mV dec⁻¹).

The long-term stability was examined by chronoamperometric response at -0.4 V (vs.

RHE) up to 60 h. The corresponding LSVs before and after stability testing were collected for comparison purpose.

The electrochemical specific surface area (ECSA) of Fe nanochain and Fe nanoparticle were obtained by CV methods.^[1] The data was collected at different scan rates from 60 to 140 mV s⁻¹. The plots of current difference ($\Delta J = J_a - J_c$) against scan rates were nearly linear and the double-layer capacitance (C_{dl} , mF cm⁻²) was obtained. In detail, the ECSA value can be calculated by the following formula:

$$\text{ECSA} = C_{dl}/C_s$$

Where $C_s = 0.035$ mF cm⁻² (the benchmark value).

2. Calculations for NH₃ yield rates and Faradaic efficiency (FE)

The detailed NH₃ yield rates have been calculated by using the following equation:

$$Y(\text{NH}_3) = [(c(\text{cathode}, \text{N}_2) - c(\text{cathode}, \text{Ar})) \times V_{\text{cathode}} + (c(\text{anode}, \text{N}_2) - c(\text{anode}, \text{Ar})) \times V_{\text{anode}} + (c(\text{end gas}, \text{N}_2) - c(\text{end gas}, \text{Ar})) \times V_{\text{end gas}} + (c(\text{membrane}, \text{N}_2) - c(\text{membrane}, \text{Ar})) \times V_{\text{membrane}}] / (t \times m)$$

And the detailed FEs have been calculated as follows:

$$FE = 3F \times [(c(\text{cathode}, \text{N}_2) - c(\text{cathode}, \text{Ar})) \times V_{\text{cathode}} + (c(\text{anode}, \text{N}_2) - c(\text{anode}, \text{Ar})) \times V_{\text{anode}} + (c(\text{end gas}, \text{N}_2) - c(\text{end gas}, \text{Ar})) \times V_{\text{end gas}} + (c(\text{membrane}, \text{N}_2) - c(\text{membrane}, \text{Ar})) \times V_{\text{membrane}}] / (17 \times Q)$$

where $c(\text{cathode}, \text{N}_2)$, $c(\text{anode}, \text{N}_2)$, $c(\text{end gas}, \text{N}_2)$ and $c(\text{membrane}, \text{N}_2)$ is NH₃ concentrations of N₂ as the feed gas in the cathode, anode, end gas and membrane chamber, $c(\text{cathode}, \text{Ar})$, $c(\text{anode}, \text{Ar})$, $c(\text{end gas}, \text{Ar})$ and $c(\text{membrane}, \text{Ar})$ is NH₃

concentration of Ar as the feed gas in the cathode, anode, end gas and membrane chamber, F is Faradaic constant, $V_{cathode}$, V_{anode} , $V_{end\ gas}$ and $V_{membrane}$ is the volume of corresponding electrolyte, t is reaction time, and m is catalyst mass.

3. Determination of NH_3 product by indophenol blue method

3.1 Preparation of chromogenic reagents: 2 mL of 1 M NaOH aqueous solution was dissolved in 5 wt% of sodium citrate and 5 wt% of salicylic acid and labelled as solution **A**. 1 mL of 0.05 M NaClO aqueous solution was labelled as solution **B**. 0.2 mL of 1 wt% $\text{C}_5\text{FeN}_6\text{Na}_2\text{O}$ aqueous solution was labelled as solution **C**.

3.2 Preparation of test solutions: After chronoamperometric test, the cathode solution, anode solution, and exhaust gas absorption liquid were collected for the chromogenic test. In addition, the Nafion 115 membrane was soaked in 5 mL of 0.5 M sulfuric acid aqueous solution for 24 h and diluted to 50 mL for the chromogenic test.

3.3 UV-vis absorption spectrum measurement: Firstly, 2 mL of above test solution was mixed with color reagents **A**, **B** and **C** successively. Next, the mixed solution was left in dark under ambient condition for 2 h, and then subjected to UV-vis measurement in the absorption peak range of 550-750 nm. The amount of NH_3 was determined by comparing the UV-vis peaks of Ar and N_2 -saturated systems.

II. Supplementary Results

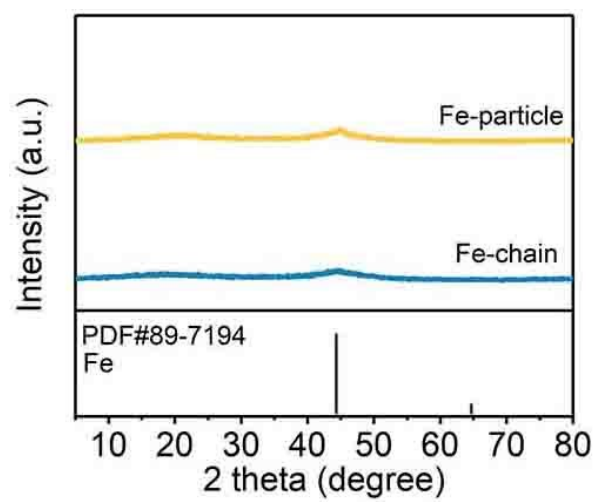


Figure S1. XRD patterns of amorphous Fe nanochains and Fe nanoparticles.

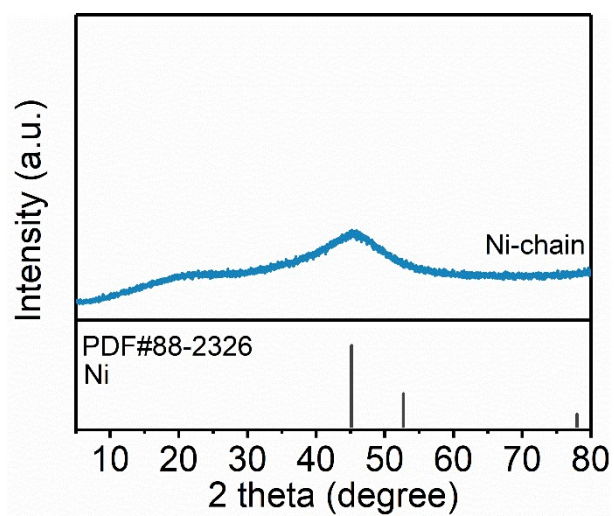


Figure S2. XRD patterns of amorphous Ni-chain.

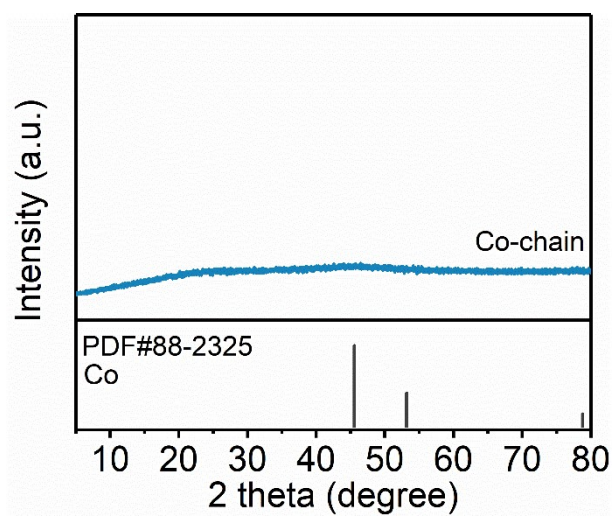


Figure S3. XRD patterns of amorphous Co-chain.

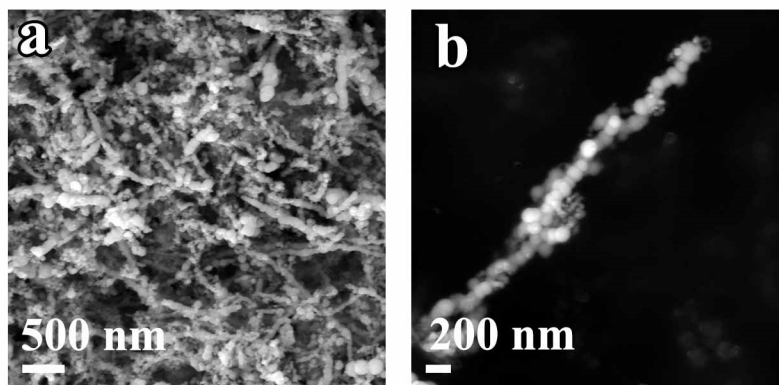


Figure S4. SEM images of amorphous Ni-chain (scale bars for a and b are 500 nm and 200 nm).

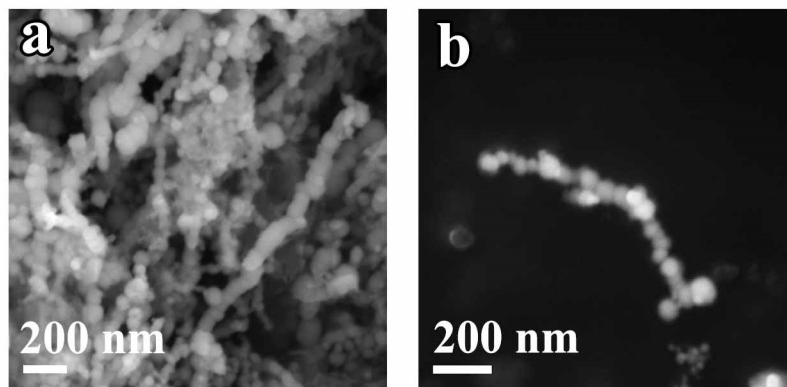


Figure S5. SEM images of amorphous Co nanochain.

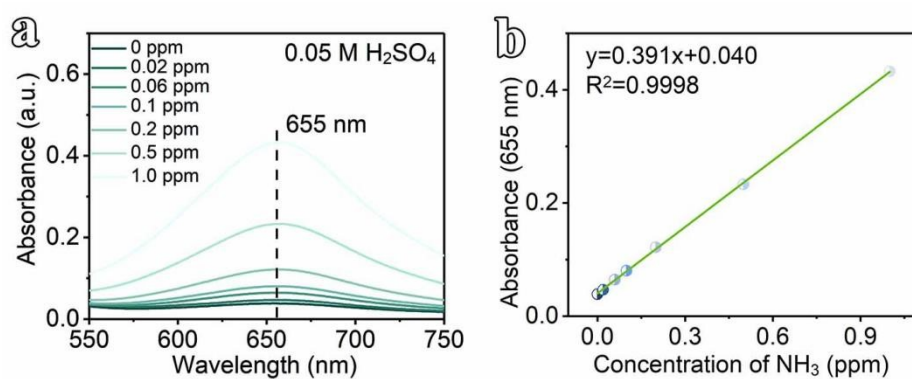


Figure S6. Calibration curves for NH₄Cl in 0.05 M H₂SO₄ solution. (a) UV-vis absorption spectra. (b) the calibration curve.

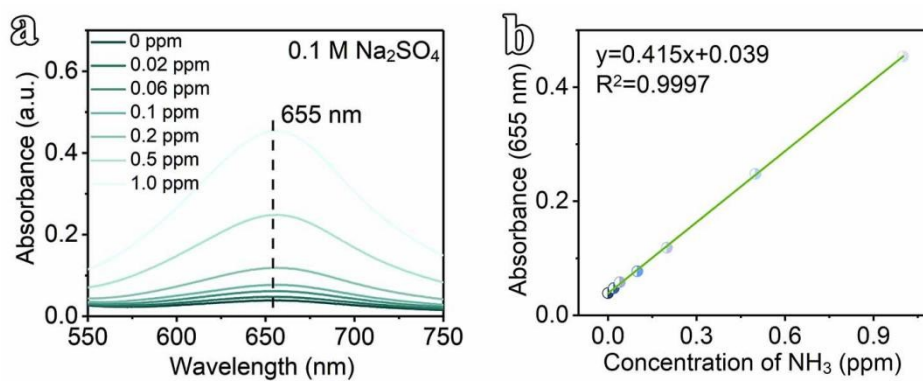


Figure S7. Calibration curves for NH_4Cl in $0.1 \text{ M Na}_2\text{SO}_4$ solution. (a) UV-vis absorption spectra. (b) the calibration curve.

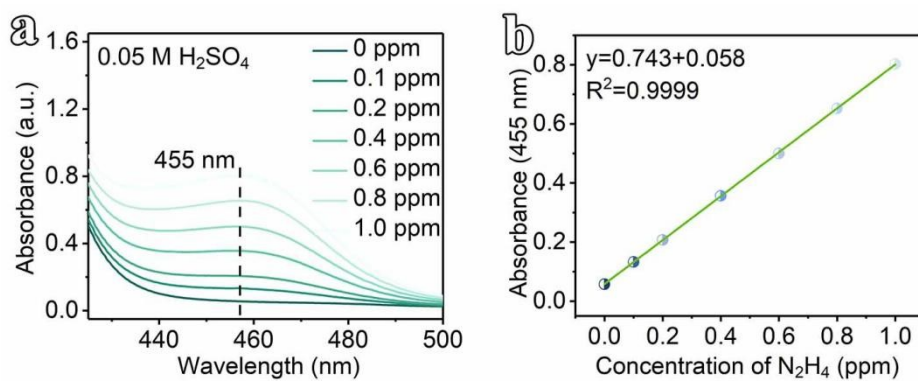


Figure S8. Calibration curves for N_2H_4 in $0.05\text{ M H}_2\text{SO}_4$ solution. (a) UV-vis absorption spectra. (b) the calibration curve.

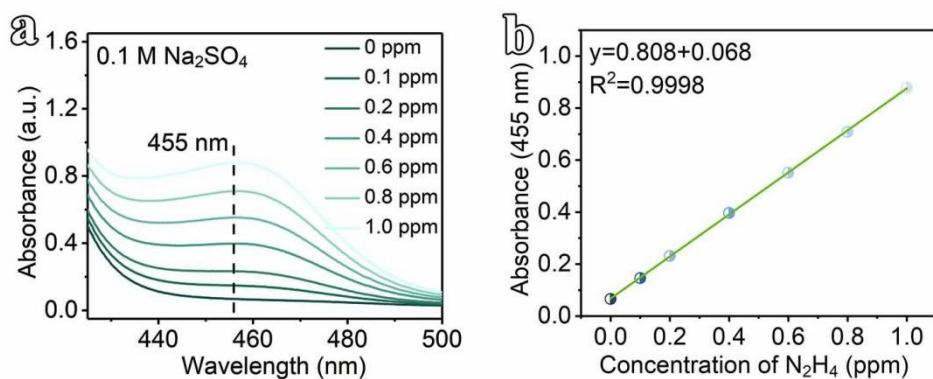


Figure S9. Calibration curves for N_2H_4 in $0.1 \text{ M Na}_2\text{SO}_4$ solution. (a) UV-vis absorption spectra. (b) the calibration curve.

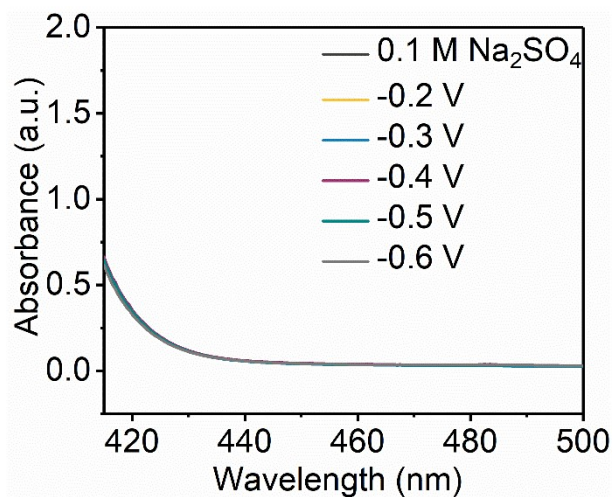


Figure S10. Watt-Chrisp method to determine the possible hydrazine by-product using Fe-chain as the NRR electrocatalyst after 1 hr electrolysis in N₂-saturated 0.1 M Na₂SO₄ solution. All UV-vis curves show no peak at 455 nm, indicating that no hydrazine is produced during the reaction process.

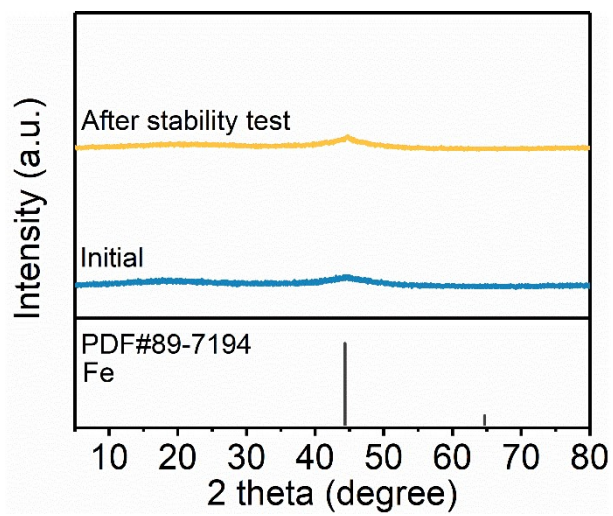


Figure S11. XRD patterns of Fe-chain electrode after stability test.

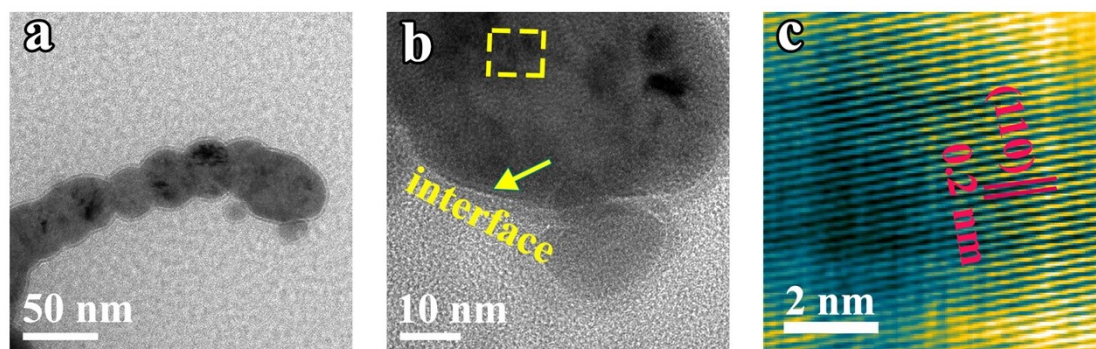


Figure S12. Morphological characterizations of Fe nanochains electrode after stability test. (a) TEM image; (b) HR-TEM image; (c) Selected area magnified HR-TEM image.

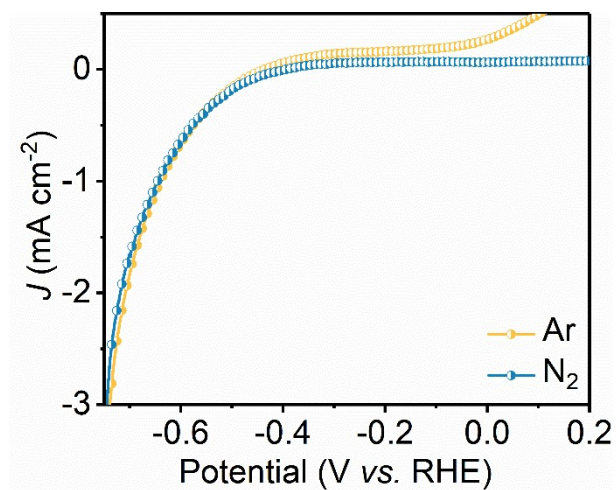


Figure S13. The LSVs of Fe-particle at the different potentials in N₂-saturated 0.1 M Na₂SO₄ electrolyte.

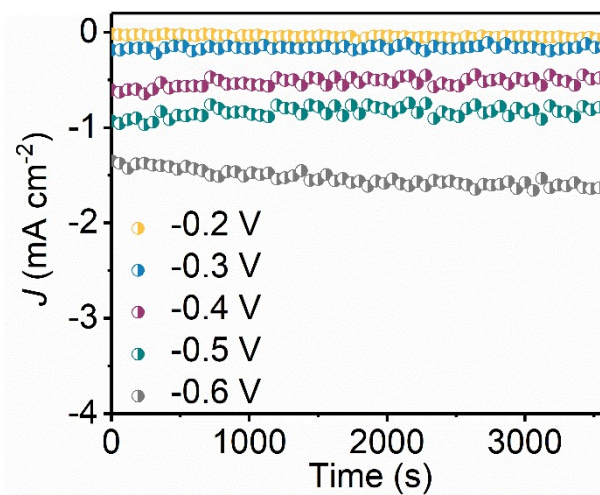


Figure S14. The chronoamperometric curves of Fe-particle at different potential in N_2 -saturated 0.1 M Na_2SO_4 electrolyte.

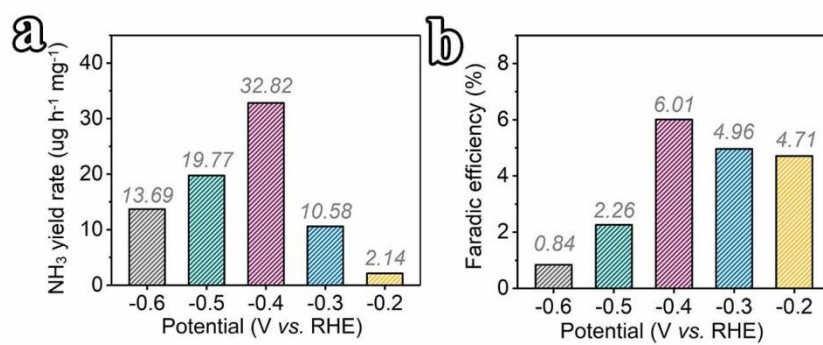


Figure S15. The NH_3 yield rates (a) and FEs (b) of Fe-particle at different potential in N_2 -saturated 0.1 M Na_2SO_4 electrolyte.

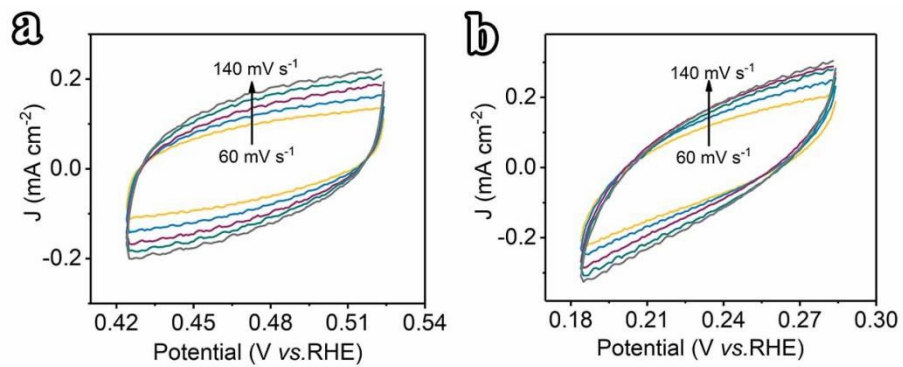


Figure S16. ECSA data for Fe-chain (a), and Fe-particle (b) at different scan rates from 60 to 140 mV s⁻¹.

Table S1. Comparison of the NRR activity for Fe nanochains with several recently reported electrocatalysts with better activity.

Catalyst	Electrolyte	Working potential (V)	NH ₃ yield rates	FE	Reference
Fe nanochains	0.1 M Na₂SO₄	-0.4	92.42 μg h⁻¹ mg⁻¹	20.02%	This work
RuFeCoNiCu/CP	0.1 M KOH	0.05	57.1 μg h ⁻¹ mg ⁻¹	38.5%	<i>Adv. Funct. Mater.</i> 2020 , <i>31</i> , 2006939.
γ-Fe ₂ O ₃	0.1 M KOH	0.0	0.21 μg h ⁻¹ mg ⁻¹	1.9%	<i>ACS Sustainable Chem. Eng.</i> 2017 , <i>5</i> , 10986.
FeSA-N-C	0.1 M KOH	0.0	7.48 μg h ⁻¹ mg ⁻¹	56.55%	<i>Nat. Commun.</i> 2019 , <i>10</i> , 341.
NiFe-MOF	0.1 M NaHCO ₃	-0.345	9.3 μg h ⁻¹ mg ⁻¹	11.5%	<i>J. Mater. Chem. A</i> 2020 , <i>8</i> , 3658.
NiFe-nanomesh array	0.1 M Na ₂ SO ₄	-0.35	16.89 μg h ⁻¹ mg ⁻¹	12.5%	<i>ACS Catal.</i> 2020 , <i>10</i> , 11371.
NiFe-nanomesh	0.1 M Na ₂ SO ₄	-0.35	4.2 μg h ⁻¹ mg ⁻¹	10.68%	<i>ACS Catal.</i> 2020 , <i>10</i> , 11371.
Co ₃ Fe-MOF	0.1 M KOH	-0.20	8.79 μg h ⁻¹ mg ⁻¹	25.64%	<i>J. Mater. Chem. A</i> 2020 , <i>8</i> , 3658.

Journal Name		COMMUNICATION			
					<i>ACS</i>
Fe _{3%} -Cu _{2-x} S QDs	0.1 M Na ₂ SO ₄	-0.7	26.4 μg h ⁻¹ cm ⁻²	3.1%	<i>Sustainable Chem. Eng.</i> 2021 , <i>9</i> , 2844.
Au/Fe ₂ (MoO ₄) ₃	0.2 M Na ₂ SO ₄	-0.4	7.61 μg h ⁻¹ mg ⁻¹	18.79%	<i>Adv. Energy Mater.</i> 2021 , <i>11</i> , 2003701.
FeSA-NO-C-900	0.1 M HCl	-0.4	31.8 μg h ⁻¹ mg ⁻¹	11.8%	<i>Angew. Chem. Int. Ed.</i> 2021 , <i>60</i> , 9078.
Fe-N/C-CNTs	0.1 M KOH	-0.2	34.83 μg h ⁻¹ mg ⁻¹	9.28%	<i>ACS Catal.</i> 2018 , <i>9</i> , 336.
Fe-MoS ₂ /CC	0.1 M KOH	-0.1	12.5 μg h ⁻¹ mg ⁻¹	10.8%	<i>Nano Energy</i> 2019 , <i>62</i> , 282.
Fe ₃ O ₄ /Ti	0.1 M Na ₂ SO ₄	-0.4	5.60×10 ⁻¹¹ mol h ⁻¹ cm ⁻²	2.6%	<i>Nanoscale</i> 2018 , <i>10</i> , 14386.
NiFe ₂ O ₄ /RGO	0.5 M LiClO ₄	-0.5	32.2 μg h ⁻¹ mg ⁻¹	9.8%	<i>Dalton Trans.</i> 2020 , <i>49</i> , 12559.
Fe/Fe ₃ O ₄	0.1 M PBS	-0.30	0.19 μg h ⁻¹ mg ⁻¹	8.29%	<i>ACS Catal.</i> 2018 , <i>8</i> , 9312.
Au/Fe ₃ O ₄	0.1 M KOH	-0.2	21.42 μg h ⁻¹ cm ⁻²	10.54%	<i>Adv. Funct. Mater.</i> 2019 , <i>30</i> , 1906579.

References

- [1] Y. Sun, S. Ding, C. Zhang, J. Duan and S. Chen, *J. Mater. Chem. A* 2021, **9**, 1603.